Flux roughening in spin ice with mixed $\pm J$ interactions

Masaki Kato,[1] Hiroyasu Matsuura,[1] Masafumi Udagawa,[2] and Masao Ogata[1,3]
[1]*Department of Physics, University of Tokyo, Hongo, Bunkyo-ku, Tokyo 113-0033, Japan*
[2]*Department of Physics, Gakushuin University, Mejiro, Toshima-ku, Tokyo 171-8588, Japan*
[3]*Trans-Scale Quantum Science Institute, University of Tokyo, Bunkyo, Tokyo 113-0033, Japan*

(Received 15 April 2022; revised 8 July 2022; accepted 11 July 2022; published 28 July 2022)

Spin ice presents a typical example of a classical spin liquid, where conserved magnetic fluxes emerge from microscopic spin degrees of freedom. In this paper, we investigate the effect of perturbation by magnetic charge disorder in two-dimensional spin ice. To this aim, we develop a cluster update algorithm which enables fast relaxation of magnetic charges. The efficient Monte Carlo calculation reveals a drastic change of the spin structure factor as doping magnetic charges: the pinch point, characterizing the spin ice, is gradually replaced by a diffusive peak. We derive an analytical relation connecting the flux fluctuation and the spin structure factor, and we explain the evolution of the diffusive peak in terms of the roughening of magnetic fluxes.

DOI: 10.1103/PhysRevB.106.014423

I. INTRODUCTION

Recently, quantum and classical spin liquids have attracted considerable attention due to their exotic properties and potential application to information devices [1–3]. The unusual properties of spin liquids are attributed to the nonlocal nature of these systems: global objects, such as fluxes and vortices, emerge from microscopic spin degrees of freedom [4–7]. They act as a main carrier of energy and information to produce many unusual features of the system [8–24].

Spin ice gives a typical example of a classical spin liquid, which now has a long history of intensive research [25]. In spin ice, spins satisfy a strict local constraint of the 2-in 2-out ice rule, which can be mapped to a global magnetic flux under a Gauss's law. This flux picture provides a systematic description of many aspects of spin ice, such as the origin of singularity in the magnetic structure factor known as a pinch point [26,27]. Moreover, one can associate a winding number with the flux itself and make a topological classification of degenerate ground states. The notion of flux is also useful to the computational and memory device application of artificial spin ice [28–30].

Given these crucial roles of the magnetic fluxes, its response to external perturbation is of natural interest. In general, the information stored in nonlocal objects is robust against local perturbations. On one hand, this robustness is favorable for the purpose of, e.g., memory storage, since the stored information is hard to dissipate. On the other hand, the robustness results in difficulty in manipulation, since one usually uses local probes to control information. These conflicting aspects require us to sophisticate our knowledge: it is crucial to classify the response of magnetic fluxes according to the types of external perturbations.

One remarkable case study in this direction is the introduction of nonmagnetic impurities or spin vacancies [31–37]. Vacancies unexpectedly introduce emergent dipoles in spin ice as a result of fractionalization, which serve as effective low-energy degrees of freedom, leading to a topological glassy state [34]. In this paper, we examine another possibility of perturbation by magnetic charge disorder induced by ferromagnetic interactions. This setting may be relevant to the application of spin ice to memory devices for computation, since the induced magnetic charges may be used as elemental bits, storing binary information as the sign of charges. The system with mixed interaction signs may also be relevant in considering a class of pyrochlore oxides, such as iridates [38–49], where the interaction between rare-earth moments are in a subtle competition between ferromagnetic and antiferromagnetic [38].

In this paper, we consider the two-dimensional spin-ice model, i.e., the nearest-neighbor antiferromagnetic Ising model on a checkerboard lattice with a certain fraction of ferromagnetic plaquettes. The magnetic charges induced on ferromagnetic plaquettes cause a severe difficulty of slow relaxation. To overcome this problem, we develop an algorithm, which we name the zero-energy cluster (ZEC) update. This algorithm enables us to explore the gradual destruction of spin ice by the induced magnetic charges. We find that the collapse of spin ice is characterized by the evolution of the magnetic structure factor: the iconic pinch point of spin ice is replaced by a diffusive peak. We derive an analytical relation between the magnetic flux fluctuation and the structure factor at a special wave number, and we find that a flux roughening causes this instability of spin ice.

II. MODEL

We consider the nearest-neighbor Ising model on a checkerboard lattice of $N_{\rm P} \equiv N \times N$ plaquettes (squares with diagonals) with periodic boundary conditions. Ising spins $\sigma_j = \pm 1$ are placed on all $N_{\rm site} \equiv 2N_{\rm P}$ lattice points [Fig. 1(a)]. If we consider plaquette-dependent interactions,

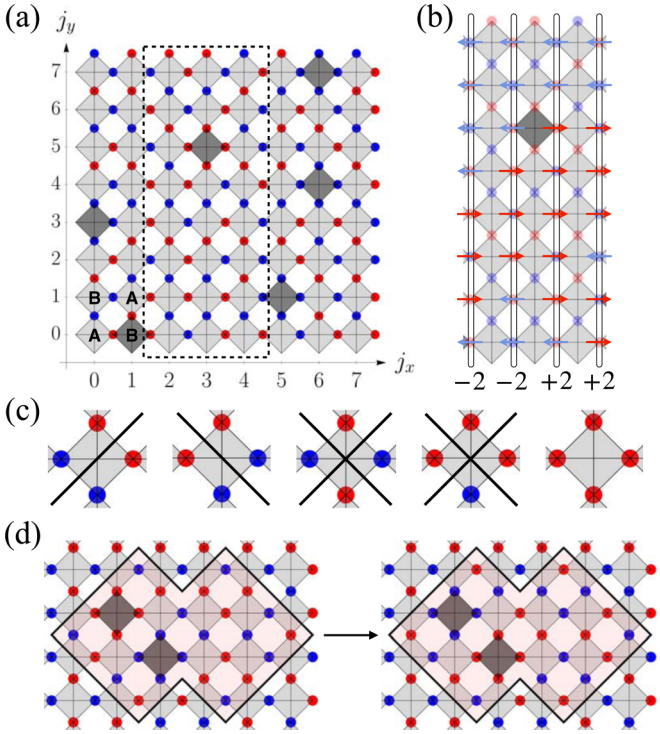

FIG. 1. (a) The lattice geometry is shown for $N = 8$. A checkerboard lattice is placed on the x-y plane, with the origin at the left-bottom plaquette. The space between neighboring plaquettes is set to be 1: The plaquettes are located at $\boldsymbol{R}_p = (j_x, j_y)$, and the spins are located at $\boldsymbol{r}_j = (j_x, j_y + \frac{1}{2})$ and $(j_x + \frac{1}{2}, j_y)$ with integers $0 \leqslant j_x, j_y \leqslant N - 1$. One of the ground states of Hamiltonian (1) is shown here. The red (blue) circles represent $\sigma_j = +1$ (-1). The light (dark) gray plaquettes have antiferromagnetic (ferromagnetic) interactions: $J_p = +1$ (-1). The plaquettes are classified into two sublattices, A and B. (b) Arrow representation for the spin configuration in a dashed box in panel (a). Right-directed (left-directed) arrows are depicted in red (blue). The numbers at the bottom show W^x_{jx} = (the number of $\rightarrow$) - (the number of $\leftarrow$) on a line separating two plaquette columns at $x = j_x$ and $j_x + 1$. On both sides of the central column, W^x_{jx} changes by 4, due to the ferromagnetic plaquette supporting a charge $Q_p = 4$. (c) Examples of bonds drawn in the ZEC update. (d) Example of a closed region separated by bonds in the ZEC update.

the Hamiltonian reads

$$\mathcal{H} = \sum_{\langle i,j \rangle} J_{ij}\sigma_i\sigma_j = \frac{1}{2}\sum_p J_p Q_p^2 + \text{Const.} \tag{1}$$

On each plaquette p, we have introduced a magnetic charge $Q_p \equiv \eta_p \sum_{i\in p}\sigma_i$. The sign factor η_p takes $+1$ (-1) on the sublattice A (B) of plaquette p [Fig. 1(a)], which is essential to make Q_p a conserved charge.

If $J_p > 0$, Hamiltonian (1) immediately results in the ice rule $Q_p = 0$ at the ground state, which leaves macroscopic degeneracy [50,51]. In this work, we choose J_p randomly according to the binary distribution $P(J_p)$:

$$J_p = \begin{cases} -J & P(-J) = p_{\mathrm{F}}, \\ J & P(+J) = 1 - p_{\mathrm{F}}. \end{cases} \tag{2}$$

p_{F} denotes a fraction of ferromagnetic plaquettes: $p_{\mathrm{F}} = 0$ (1) corresponds to the checkerboard spin ice (pure ferromagnetic Ising model).

The ferromagnetic plaquettes induce finite magnetic charges at low temperatures. At least for a small number of ferromagnetic plaquettes, the ground state keeps macroscopic degeneracy, satisfying a modified ice rule: $Q_p = 0$ (± 4) for antiferromagnetic (ferromagnetic) plaquettes. A convenient illustrative method to describe this modified ice rule is the arrow representation: replace a spin $\sigma_j = +1$ (-1) with an arrow pointing from the plaquette of A (B) sublattice to B (A) sublattice [Fig. 1(b)]. In this expression, each ground state corresponds to a configuration of a six-vertex model with all-in/all-out vertices of ferromagnetic plaquettes. This expression is also suitable for the formulation of the columnar transfer matrix to calculate the observables at the ground state.

Another advantage of the arrow representation is that we can visualize a conserved magnetic flux [Fig. 1(b)]. To see this, let us draw a line parallel to the y axis between two adjacent columns of plaquettes. We define $W^x_{j_x}$ as the difference between the number of right-directed arrows and that of left-directed arrows on the line. The magnetic flux is conserved in a sense that $W^x_{j_x}$ does not depend on the position of the line as long as $Q_p = 0$ is satisfied. More precisely, the magnetic charge Q_p serves as a source of the flux: When a finite charge Q_p exists, the value of $W^x_{j_x}$ changes by Q_p. In this sense, $W^x_{j_x}$ deserves the name of "magnetic flux." We will come back to a formal definition of magnetic flux and its relation to an observable quantity later.

III. METHOD

We study the low-temperature property of Hamiltonian (1) by the Monte Carlo method. In the simulation of spin-ice-type models, the loop update algorithm is usually available to accelerate relaxation at low temperatures [52–54], and similar algorithms are also applied to dimer models [55,56], vertex models [57], and loop models [58]. These update methods, however, do not work for the relaxation of magnetic charges. The basic idea of the loop update is to find a tensionless loop by Brownian motion, which premises the ice rule and is effective only in the spin-ice manifold. A variant of the loop update was also proposed to transfer a charge along a string connecting positive and negative charges [59]. However, this algorithm is also ineffective for the present purpose, since the stable charge values of ferromagnetic plaquettes are well separated, $Q_p = \pm 4$. With this charge transfer algorithm, we need to transfer $\Delta Q = 8$ by finding four strings connecting a charge pair, which inevitably make the program code extremely cumbersome.

Considering these difficulties in the string-based algorithms, we turn our attention to a cluster rather than a string and propose the ZEC update as introduced below. The basic idea of the ZEC update is to find a cluster of spins flippable without any energy cost. By repeating cluster flips that contain different sets of magnetic charges, one can relax charges efficiently. The protocol of the ZEC update is simply summarized as follows:

(i) Draw a bond on each plaquette if the interactions across the bond sum up to zero [Fig. 1(c)].

(ii) Choose a closed region surrounded by the bonds and flip all the spins inside the boundary [Fig. 1(d)].

In step (i), we must select the bonds on only one of the two sublattices of the dual square lattice; otherwise, the detailed balance condition is violated. For details of this point and for practical information, such as the procedure to identify the boundaries, see the Supplemental Material [60]. A similar cluster construction based on the dual-lattice formulation has been proposed for different models [58,61–63]. In the following, we use the ZEC update in parallel with the single spin update based on the heat bath algorithm and the loop update.

IV. BENCHMARK

To justify our algorithm, we show the comparison with the exact transfer matrix calculation for a small system of 20×10 plaquettes with a periodic array of ferromagnetic plaquettes [inset of Fig. 2(a)]. Figure 2(a) shows the charge correlation on ferromagnetic plaquettes $[\langle Q_p Q_{p'}\rangle]$ for three different methods: transfer matrix (red), the Monte Carlo method with the ZEC update (blue), and the Monte Carlo method without the ZEC update (green). The conventional algorithm leads to substantial deviation even for this size of small cluster. With the ZEC update, the difference from the exact result is within the error bar of Monte Carlo sampling. We have made comparisons for a variety of periodic charge patterns and found that the ZEC update gives accurate results up to $p_{\rm F} \lesssim 0.2$. The ZEC update is still useful above this upper bound to some extent. Yet certain local arrangements of ferromagnetic plaquettes interrupt the performance of this algorithm. For this problem, see the Supplemental Material [60].

To demonstrate the efficiency of the ZEC update for fast relaxation, we compute the spin and charge autocorrelation functions defined as $\Phi(t) \equiv |[\frac{1}{N_{\rm site}}\sum_i \langle\sigma_i(0)\sigma_i(t)\rangle]|$ and $\Phi_{\rm Q}(t) \equiv |[\frac{1}{N_{\rm F}}\sum_{p\in\boxtimes_{\rm F}}\langle Q_p(0)Q_p(t)\rangle]|$, respectively, with t being the Monte Carlo steps after the equilibration. Here, $\langle\cdots\rangle$ and $[\cdots]$ denote the thermal average and the random average over the configurations of ferromagnetic plaquettes, respectively. Note that the charge correlation is defined for the ferromagnetic plaquettes. Figures 2(b) and 2(c) show $\Phi(t)$ and $\Phi_{\rm Q}(t)$ calculated for $N_{\rm P} = 10^4$ and $p_{\rm F} = 0.1$ and 0.2 at $T/J = 10^{-2}$, with and without the ZEC update. Figure 2(b) clearly shows that the ZEC update improves the spin relaxation considerably. With only single and loop updates, $\Phi(t)$ stays $\sim$0.4 (0.6) for $p_{\rm F} = 0.1$ (0.2) after a long time. With the ZEC update, $\Phi(t)$ quickly falls off to the correct value near $\sim$0. This tendency is clearer in the charge relaxation, as shown in Fig. 2(c). Without the ZEC update, the charge autocorrelation does not show the slightest sign of relaxation and keeps the value $\sim$1. This persistence of magnetic charge is quickly improved by the introduction of the ZEC update.

We also remark on the characteristic relaxation process in the ZEC update algorithm. In the insets of Figs. 2(b) and 2(c), we show the logarithmic plots of $-\ln\Phi(t)$ and $-\ln\Phi_{\rm Q}(t)$, respectively. Towards the equilibrium values, they show nearly linear behavior; i.e., the relaxation process can be fitted by a stretched exponential, $\sim\exp[-(t/\tau)^\beta]$, with β being dependent on the value of $p_{\rm F}$. The stretched exponential relaxation is often discussed in glasses and highly frustrated systems [64,65], where a complex hierarchy of energy scales is suspected. The cluster sizes flipped through the ZEC update also make a complex distribution, which may underlie this nontrivial relaxation dynamics.

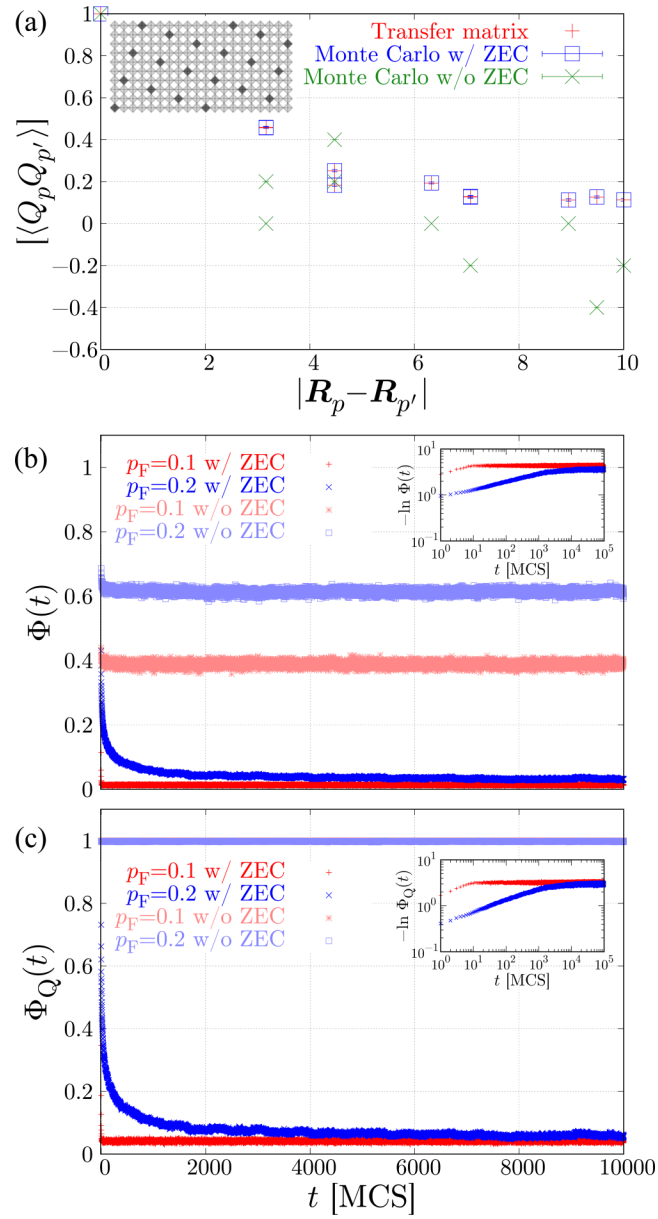

FIG. 2. (a) Comparisons of the charge correlation $[\langle Q_p Q_{p'}\rangle]$ on ferromagnetic plaquettes p and p' between the exact transfer matrix method and the Monte Carlo simulation with and without the ZEC update, for the periodic array of ferromagnetic plaquettes embedded in the checkerboard lattice of 20×10 plaquettes, as shown in the inset. (b) $\Phi(t)$ and (c) $\Phi_{\rm Q}(t)$ for $p_{\rm F} = 0.1$ and 0.2 with and without the ZEC update. The insets show (b) $-\ln\Phi(t)$ and (c) $-\ln\Phi_{\rm Q}(t)$.

V. STRUCTURE FACTOR

We now investigate the physical properties of the system using the ZEC update algorithm. As a physical observable, we focus on the spin structure factor $S(\boldsymbol{q}) = [\langle\sigma_{-\boldsymbol{q}}\sigma_{\boldsymbol{q}}\rangle]$, where $\sigma_{\boldsymbol{q}} \equiv \frac{1}{\sqrt{N_{\rm site}}}\sum_j \sigma_j e^{i\boldsymbol{q}\cdot\boldsymbol{r}_j}$. Figure 3 shows $S(\boldsymbol{q})$ obtained by the Monte Carlo simulation for $N_{\rm p} = 10^4$ for different fractions

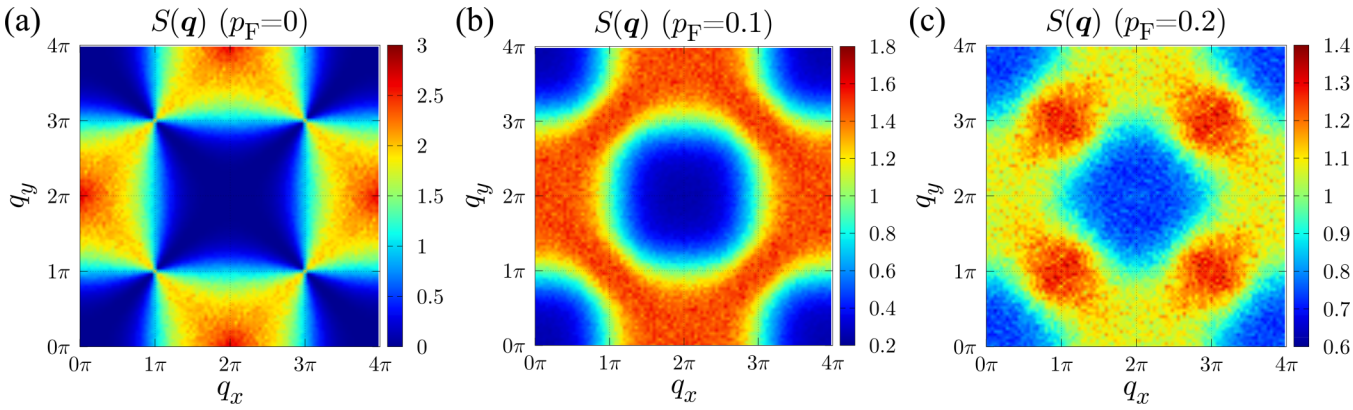

FIG. 3. The magnetic structure factor $S(\boldsymbol{q})$ calculated by Monte Carlo simulation for $N_P = 10^4$ for (a) $p_F = 0$, (b) $p_F = 0.1$, and (c) $p_F = 0.2$.

of ferromagnetic plaquettes at the temperature $T/J = 10^{-2}$. At $p_F = 0$, all the plaquettes are antiferromagnetic, and the system forms a perfect spin ice at zero temperature. Reflecting the spin-ice formation, $S(\boldsymbol{q})$ exhibits a singularity at $\boldsymbol{q} = \boldsymbol{q}_p \equiv (\pi, \pi)$ and equivalent wave numbers [Fig. 3(a)]. This is the pinch point, an iconic character of spin ice, reflecting the divergence-free nature of magnetic fluxes [26,27].

As the number of ferromagnetic plaquettes increases, the ice rule is gradually modified. As shown in Fig. 3(b), the pinch point quickly blurs and is replaced by a ridgelike structure, which is reminiscent of the neutron scattering images for several spin-ice candidate materials [66–69]. As the fraction of ferromagnetic plaquettes is further increased [Fig. 3(c)], even a broad peak develops at $\boldsymbol{q}_p$ where the pinch point was originally placed. In general, the destruction of the pinch point reflects the instability of spin ice, and the structural change of $S(\boldsymbol{q})$ around $\boldsymbol{q}_p$ is used to classify the type of instability [59,69–73]. However, to our knowledge, the growth of a peak at $\boldsymbol{q}_p$ has rarely been reported either in theories or in experiments on classical spin ice, with a possible exception in a three-dimensional quantum spin-ice candidate system [74].

VI. MAGNETIC FLUXES

Actually, the value of $S(\boldsymbol{q}_p)$ carries important information on the nonlocal property of the system as discussed below. This wave number, $\boldsymbol{q}_p = (\pi, \pi)$, has already drawn attention as the place of the singular pinch point. However, here we would like to focus on the value of $S(\boldsymbol{q}_p)$ itself. Indeed, even after the spin ice is destroyed and the singularity is washed away, $S(\boldsymbol{q}_p)$ stores important information on the global fluxes of the system. This relation also gives a precious example in which nonlocal character of the system can be accessed through local observables [75,76].

To clarify the connection between the magnetic fluxes and $S(\boldsymbol{q}_p)$, we write the formal expression of magnetic flux as

$$W^x_{jx} = \sum_{j_y} (-1)^{j_x+j_y} \sigma_{j_x+1/2, j_y},$$
$$W^y_{j_y} = \sum_{jx} (-1)^{j_x+j_y} \sigma_{j_x, j_y+1/2}. \quad (3)$$

This expression is equivalent to the intuitive arrow counting presented in Fig. 1(b). In the expression (3), $(-1)^{j_x+j_y}$ is a sign factor to distinguish A and B sublattices of the plaquettes [Fig. 1(a)]. This factor is in turn translated into a phase factor at $\boldsymbol{q}_p = (\pi, \pi)$. We obtain $\sigma_{\boldsymbol{q}_p} = \frac{1}{\sqrt{N_{site}}}(\sum_{jx} W^x_{jx} + \sum_{j_y} W^y_{j_y})$ up to a constant phase, which leads to the relation

$$S(\boldsymbol{q}_p) = [\langle (W^x)^2 \rangle] = [\langle (W^y)^2 \rangle], \quad (4)$$

where $W^x = \frac{1}{N}\sum_{jx} W^x_{jx}$ and $W^y = \frac{1}{N}\sum_{j_y} W^y_{j_y}$. This claims that $S(\boldsymbol{q}_p)$ is proportional to the fluctuation of the global magnetic fluxes.

In terms of Eq. (4), it is possible to attribute the evolution of the structure factor to the enhanced fluctuation of the magnetic fluxes. In the absence of ferromagnetic plaquettes, the flux value is uniform over the system, and the zero-flux configurations have the largest weight. Finite-flux configurations occur only occasionally over the Monte Carlo steps. In the presence of ferromagnetic plaquettes, however, the nature of the flux fluctuation qualitatively changes: The fluctuation becomes "spatial" rather than "temporal." In Fig. 4, we show the snapshot of the flux distribution. As is clearly seen here, the flux $(W^x_{jx}, W^y_{j_y})$ changes its value at ferromagnetic plaquettes, producing a mosaic pattern. The accumulated charges $Q_p = \pm 4$ on the ferromagnetic plaquettes force the flux value to change by 4. As the fraction of ferromagnetic plaquettes increases, the flux distribution shows roughening: This enhanced spatial fluctuation of the magnetic fluxes is observed as the diffusive peak of $S(\boldsymbol{q})$ at $\boldsymbol{q} = \boldsymbol{q}_p$.

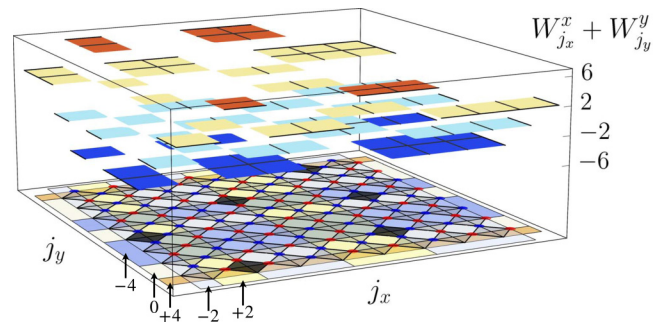

FIG. 4. Snapshot of the set of the magnetic fluxes $(W^x_{jx}, W^y_{j_y})$ and their sum $W^x_{jx} + W^y_{j_y}$. In the presence of charges, the flux varies spatially and its pattern looks like a mosaic exhibiting spatial roughening.

VII. SUMMARY AND DISCUSSIONS

In summary, we have studied the effect of perturbation by magnetic charge disorder in spin ice, by taking the model of a checkerboard lattice with mixed $\pm J$ plaquette interactions. For the relaxation of magnetic charges, we have developed a type of cluster update algorithm for the Monte Carlo simulation called ZEC. This numerical innovation enabled us to explore the gradual collapse of spin ice by increasing ferromagnetic plaquettes, which is signaled by the replacement of the pinch point by a diffusive peak. The evolution of the diffusive peak is attributed to the flux roughening, which is verified on the basis of a firm relation between the flux fluctuation and the spin structure factor at $\boldsymbol{q}_{\rm p} = (\pi, \pi)$.

The present study can be extended to many directions. The collapse of the pinch point structure has been used to classify the instabilities of spin ice. This theoretical finding must be useful to interpret future experiments. For example, in pyrochlore iridates, keen competition of ferromagnetic and antiferromagnetic interactions has been actively debated. While the number of available neutron scattering data is limited due to the notoriously high neutron absorption rate of Ir, it is interesting to look for the signature of competing interactions in $S(\boldsymbol{q})$ at finite temperatures.

It is also interesting to proceed with our analysis to larger $p_{\rm F}$, where we expect that the flux roughening shows further enhancement. If the density of ferromagnetic plaquettes increases, the system cannot satisfy the modified ice rule any more and faces severe frustration. There, the appearance of a complex energy landscape is naturally expected, which may give rise to a new type of topological glassy state.

From the technical viewpoint, our ZEC update provides a powerful tool to analyze systems suffering slow relaxation. For instance, it is important to apply this algorithm to spin glass models and other types of spin-ice-like systems [77–81], in which slow relaxation always confronts us. Our algorithm can be flexibly extended to higher-dimensional systems or to include different degrees of freedom. We would like to leave these fascinating problems for future work.

ACKNOWLEDGMENTS

This work was supported by JSPS KAKENHI (Grants No. JP20H05655, No. JP20H04463, and No. JP22H01147), MEXT, Japan. M.K. was supported by JSPS through the Program for Leading Graduate Schools (MERIT-WINGS).

[1] J. K. Pachos, *Introduction to Topological Quantum Computation* (Cambridge University Press, Cambridge, England, 2012).
[2] L. Balents, Nature (London) **464**, 199 (2010).
[3] J. Knolle and R. Moessner, Annu. Rev. Condens. Matter Phys. **10**, 451 (2019).
[4] C. Castelnovo, R. Moessner, and S. L. Sondhi, Nature (London) **451**, 42 (2008).
[5] M. Hermele, M. P. A. Fisher, and L. Balents, Phys. Rev. B **69**, 064404 (2004).
[6] D. A. Ivanov, Phys. Rev. B **70**, 094430 (2004).
[7] D. A. Ivanov, Phys. Rev. Lett. **86**, 268 (2001).
[8] M. Udagawa and R. Moessner, Phys. Rev. Lett. **122**, 117201 (2019).
[9] O. Petrova, R. Moessner, and S. L. Sondhi, Phys. Rev. B **92**, 100401(R) (2015).
[10] Y. Wan, J. Carrasquilla, and R. G. Melko, Phys. Rev. Lett. **116**, 167202 (2016).
[11] C.-J. Huang, Y. Deng, Y. Wan, and Z. Y. Meng, Phys. Rev. Lett. **120**, 167202 (2018).
[12] S. Kourtis and C. Castelnovo, Phys. Rev. B **94**, 104401 (2016).
[13] Z. Yan, Y.-C. Wang, N. Ma, Y. Qi, and Z. Y. Meng, npj Quantum Mater. **6**, 39 (2021).
[14] G. Chen, Phys. Rev. B **96**, 195127 (2017).
[15] G. Chen, Phys. Rev. B **96**, 085136 (2017).
[16] O. Hart, Y. Wan, and C. Castelnovo, Phys. Rev. B **101**, 064428 (2020).
[17] A. Szabó and C. Castelnovo, Phys. Rev. B **100**, 014417 (2019).
[18] L. Pan, N. J. Laurita, K. A. Ross, B. D. Gaulin, and N. P. Armitage, Nat. Phys. **12**, 361 (2016).
[19] Y. Tokiwa, T. Yamashita, M. Udagawa, S. Kittaka, T. Sakakibara, D. Terazawa, Y. Shimoyama, T. Terashima, Y. Yasui, T. Shibauchi, and Y. Matsuda, Nat. Commun. **7**, 10807 (2016).
[20] A. Ralko, M. Ferrero, F. Becca, D. Ivanov, and F. Mila, Phys. Rev. B **71**, 224109 (2005).
[21] A. Ralko, M. Ferrero, F. Becca, D. Ivanov, and F. Mila, Phys. Rev. B **76**, 140404(R) (2007).
[22] M. Udagawa, M. Ogata, and Z. Hiroi, J. Phys. Soc. Jpn. **71**, 2365 (2002).
[23] R. Moessner and S. L. Sondhi, Phys. Rev. B **68**, 064411 (2003).
[24] L. D. C. Jaubert and P. C. W. Holdsworth, Nat. Phys. **5**, 258 (2009).
[25] M. Udagawa and L. Jaubert, *Spin Ice* (Springer, Berlin, 2021).
[26] S. V. Isakov, K. Gregor, R. Moessner, and S. L. Sondhi, Phys. Rev. Lett. **93**, 167204 (2004).
[27] T. Fennell, P. Deen, A. Wildes, K. Schmalzl, D. Prabhakaran, A. Boothroyd, R. Aldus, D. McMorrow, and S. Bramwell, Science **326**, 415 (2009).
[28] R. F. Wang, C. Nisoli, R. S. Freitas, J. Li, W. McConville, B. J. Cooley, M. S. Lund, N. Samarth, C. Leighton, V. H. Crespi, and P. Schiffer, Nature (London) **439**, 303 (2006).
[29] S. H. Skjærvø, C. H. Marrows, R. L. Stamps, and L. J. Heyderman, Nat. Rev. Phys. **2**, 117 (2020).
[30] P. Schiffer and C. Nisoli, Appl. Phys. Lett. **118**, 110501 (2021).
[31] J. Snyder, J. S. Slusky, R. J. Cava, and P. Schiffer, Phys. Rev. B **66**, 064432 (2002).
[32] M. Kajňaková, M. Orendáč, A. Orendáčová, A. Vlček, T. Fennell, and S. Bramwell, J. Magn. Magn. Mater. **272**, E989 (2004).
[33] G. Ehlers, J. S. Gardner, C. H. Booth, M. Daniel, K. C. Kam, A. K. Cheetham, D. Antonio, H. E. Brooks, A. L. Cornelius, S. T. Bramwell, J. Lago, W. Häussler, and N. Rosov, Phys. Rev. B **73**, 174429 (2006).
[34] A. Sen and R. Moessner, Phys. Rev. Lett. **114**, 247207 (2015).
[35] J. Rehn, A. Sen, A. Andreanov, K. Damle, R. Moessner, and A. Scardicchio, Phys. Rev. B **92**, 085144 (2015).

[36] H. Otsuka, Y. Okabe, and K. Nefedev, Phys. Rev. E **97**, 042132 (2018).
[37] P. Andriushchenko, K. Soldatov, A. Peretyatko, Y. Shevchenko, K. Nefedev, H. Otsuka, and Y. Okabe, Phys. Rev. E **99**, 022138 (2019).
[38] K. Matsuhira, Y. Hinatsu, K. Tenya, H. Amitsuka, and T. Sakakibara, J. Phys. Soc. Jpn. **71**, 1576 (2002).
[39] M. Udagawa, H. Ishizuka, and Y. Motome, Phys. Rev. Lett. **108**, 066406 (2012).
[40] M. Udagawa and R. Moessner, Phys. Rev. Lett. **111**, 036602 (2013).
[41] S. Nakatsuji, Y. Machida, Y. Maeno, T. Tayama, T. Sakakibara, J. van Duijn, L. Balicas, J. N. Millican, R. T. Macaluso, and J. Y. Chan, Phys. Rev. Lett. **96**, 087204 (2006).
[42] Y. Machida, S. Nakatsuji, Y. Maeno, T. Tayama, T. Sakakibara, and S. Onoda, Phys. Rev. Lett. **98**, 057203 (2007).
[43] D. E. MacLaughlin, O. O. Bernal, L. Shu, J. Ishikawa, Y. Matsumoto, J.-J. Wen, M. Mourigal, C. Stock, G. Ehlers, C. L. Broholm, Y. Machida, K. Kimura, S. Nakatsuji, Y. Shimura, and T. Sakakibara, Phys. Rev. B **92**, 054432 (2015).
[44] K. Ueda, J. Fujioka, B.-J. Yang, J. Shiogai, A. Tsukazaki, S. Nakamura, S. Awaji, N. Nagaosa, and Y. Tokura, Phys. Rev. Lett. **115**, 056402 (2015).
[45] K. Ueda, J. Fujioka, Y. Takahashi, T. Suzuki, S. Ishiwata, Y. Taguchi, M. Kawasaki, and Y. Tokura, Phys. Rev. B **89**, 075127 (2014).
[46] K. Matsuhira, M. Tokunaga, M. Wakeshima, Y. Hinatsu, and S. Takagi, J. Phys. Soc. Jpn. **82**, 023706 (2013).
[47] K. Tomiyasu, K. Matsuhira, K. Iwasa, M. Watahiki, S. Takagi, M. Wakeshima, Y. Hinatsu, M. Yokoyama, K. Ohoyama, and K. Yamada, J. Phys. Soc. Jpn. **81**, 034709 (2012).
[48] T. Uehara, T. Ohtsuki, M. Udagawa, S. Nakatsuji, and Y. Machida, arXiv:2202.12149.
[49] M. Udagawa, SPIN **05**, 1540004 (2015).
[50] A. P. Ramirez, A. Hayashi, R. J. Cava, R. Siddharthan, and B. Shastry, Nature (London) **399**, 333 (1999).
[51] E. H. Lieb, Phys. Rev. Lett. **18**, 692 (1967).
[52] G. T. Barkema and M. E. J. Newman, Phys. Rev. E **57**, 1155 (1998).
[53] R. G. Melko, B. C. den Hertog, and M. J. P. Gingras, Phys. Rev. Lett. **87**, 067203 (2001).
[54] L. D. C. Jaubert, J. T. Chalker, P. C. W. Holdsworth, and R. Moessner, Phys. Rev. Lett. **100**, 067207 (2008).
[55] A. W. Sandvik and R. Moessner, Phys. Rev. B **73**, 144504 (2006).
[56] F. Alet, Y. Ikhlef, J. L. Jacobsen, G. Misguich, and V. Pasquier, Phys. Rev. E **74**, 041124 (2006).
[57] O. F. Syljuåsen and M. B. Zvonarev, Phys. Rev. E **70**, 016118 (2004).
[58] W. Zhang, T. M. Garoni, and Y. Deng, Nucl. Phys. B **814**, 461 (2009).
[59] T. Mizoguchi, L. D. C. Jaubert, and M. Udagawa, Phys. Rev. Lett. **119**, 077207 (2017).
[60] See Supplemental Material at http://link.aps.org/supplemental/10.1103/PhysRevB.106.014423 for practical issues and detailed information on the ZEC update. See Secs. A–D.
[61] P. Hitchcock, E. S. Sørensen, and F. Alet, Phys. Rev. E **70**, 016702 (2004).
[62] Y. Wang, H. De Sterck, and R. G. Melko, Phys. Rev. E **85**, 036704 (2012).
[63] G. Rakala and K. Damle, Phys. Rev. E **96**, 023304 (2017).
[64] C. De Dominicis, H. Orland, and F. Lainée, J. Phys. Lett. **46**, 463 (1985).
[65] D. C. Johnston, S.-H. Baek, X. Zong, F. Borsa, J. Schmalian, and S. Kondo, Phys. Rev. Lett. **95**, 176408 (2005).
[66] K. Kimura, S. Nakatsuji, J.-J. Wen, C. Broholm, M. B. Stone, E. Nishibori, and H. Sawa, Nat. Commun. **4**, 1934 (2013).
[67] S. Petit, E. Lhotel, B. Canals, M. Ciomaga Hatnean, J. Ollivier, H. Mutka, E. Ressouche, A. R. Wildes, M. R. Lees, and G. Balakrishnan, Nat. Phys. **12**, 746 (2016).
[68] S. Petit, E. Lhotel, S. Guitteny, O. Florea, J. Robert, P. Bonville, I. Mirebeau, J. Ollivier, H. Mutka, E. Ressouche, C. Decorse, M. Ciomaga Hatnean, and G. Balakrishnan, Phys. Rev. B **94**, 165153 (2016).
[69] C. Castelnovo and R. Moessner, Phys. Rev. B **99**, 121102(R) (2019).
[70] A. Sen, R. Moessner, and S. L. Sondhi, Phys. Rev. Lett. **110**, 107202 (2013).
[71] J. G. Rau and M. J. P. Gingras, Nat. Commun. **7**, 12234 (2016).
[72] M. Udagawa, L. D. C. Jaubert, C. Castelnovo, and R. Moessner, Phys. Rev. B **94**, 104416 (2016).
[73] T. Mizoguchi, L. D. C. Jaubert, R. Moessner, and M. Udagawa, Phys. Rev. B **98**, 144446 (2018).
[74] S. Petit, P. Bonville, J. Robert, C. Decorse, and I. Mirebeau, Phys. Rev. B **86**, 174403 (2012).
[75] L. D. C. Jaubert, M. J. Harris, T. Fennell, R. G. Melko, S. T. Bramwell, and P. C. W. Holdsworth, Phys. Rev. X **3**, 011014 (2013).
[76] D. M. Arroo and S. T. Bramwell, Phys. Rev. B **102**, 214427 (2020).
[77] M. Kato, K. Tokushuku, H. Matsuura, M. Udagawa, and M. Ogata, J. Phys. Soc. Jpn. **90**, 073704 (2021).
[78] W. Kosaka, Z. Liu, J. Zhang, Y. Sato, A. Hori, R. Matsuda, S. Kitagawa, and H. Miyasaka, Nat. Commun. **9**, 5420 (2018).
[79] E. J. Samuelsen and D. Semmingsen, J. Phys. Chem. Solids **38**, 1275 (1977).
[80] H. Ishizuka, Y. Motome, N. Furukawa, and S. Suzuki, Phys. Rev. B **84**, 064120 (2011).
[81] M. G. Yamada and Y. Tada, Phys. Rev. Research **2**, 043077 (2020).